ARTICLE

Hierarchically Ordered Macro–Mesoporous TiO_2–Graphene Composite Films: Improved Mass Transfer, Reduced Charge Recombination, and Their Enhanced Photocatalytic Activities

Jiang Du,[†] Xiaoyong Lai,[†] Nailiang Yang,[†] Jin Zhai,[‡] David Kisailus,[§] Fabing Su,[†] Dan Wang,[†,*] and Lei Jiang[‡]

[†]State Key Laboratory of Multi-phase Complex Systems, Institute of Process Engineering, Chinese Academy of Sciences, Beijing 100190, People's Republic of China, [‡]Beijing University of Aeronautics and Astronautics, Beijing 100191, People's Republic of China, and [§]Department of Chemical and Environmental Engineering, University of California Riverside, California 92521, United States

ABSTRACT Hierarchically ordered macro–mesoporous titania films have been produced through a confinement self-assembly method within the regular voids of a colloidal crystal with three-dimensional periodicity. Furthermore, graphene as an excellent electron-accepting and electron-transporting material has been incorporated into the hierarchically ordered macro–mesoporous titania frameworks by *in situ* reduction of graphene oxide added in the self-assembly system. Incorporation of interconnected macropores in mesoporous films improves the mass transport through the film, reduces the length of the mesopore channel, and increases the accessible surface area of the thin film, whereas the introduction of graphene effectively suppresses the charge recombination. Therefore, the significant enhancement of photocatalytic activity for degrading the methyl blue has been achieved. The apparent rate constants for macro–mesoporous titania films without and with graphene are up to 0.045 and 0.071 min^{-1}, respectively, almost 11 and 17 times higher than that for pure mesoporous titania films (0.0041 min^{-1}).

KEYWORDS: hierarchical · ordered macro–mesoporous · TiO_2–graphene film · photocatalysis · mass transport · efficient charge separation

*Address correspondence to danwang@mail.ipe.ac.cn.

Received for review October 15, 2010 and accepted December 15, 2010.

Published online December 28, 2010. 10.1021/nn102767d

Photocatalytic oxidation of organic compounds in water and air has received much attention as a promising technology for pollution abatement. Among various oxide semiconductor photocatalysts, titanium dioxide (TiO_2) has been recognized as the most suitable material for widespread environmental applications because of its strong oxidizing power, low cost, high chemical inertness, and photostability. Its performance is often enhanced by means of noble metal loading, metal ion doping, anion doping, and incorporation of electron-accepting materials, such as carbon nanotubes or graphene. These are used for expanding the light absorption range or suppressing the electron–hole recombination.[1−7]

Mesoporous TiO_2 films with ordered pores are among the best candidates as a host matrix for forming composite photocatalysts because of their homogeneous nanometer-sized pores, large surface areas, and their ability to be easily fixed, recycled, and reused.[1,2,8−10] Highly ordered mesoporous TiO_2 films with various mesostructures, such as *p6mm*,[11−13] *R3m*,[14] or *Im3m*,[13] have already been prepared using surfactants as structure-directed agents through the evaporation-induced self-assembly (EISA) route. However, the sizes of the mesopores in these films are often only several nanometers, which makes it difficult for organic molecules to diffuse through the pores effectively and excludes a large amount of the internal surface. Although the mesopore sizes could be enlarged to 14 nm by using swelling agents,[15] the improvement of accessibility is still relatively limited, simultaneously accompanied by the decrease of mesostructured order and specific surface area. An attractive alternative is to build a hierarchically porous system by constructing larger secondary pore channels within the mesoporous film, which will make pore openings more accessible and, thus, improve the diffusivity of reactants and products within the film and increase the availability of the internal surface.[16−20] Kimura *et al.* have synthesized ordered mesoporous TiO_2 films with macropores by using emulsion or polystyrene (PS) spheres as macroporous templates but had difficulty in controlling the interconnectivity and concentration of macropores.[21,22] Jin *et al.* reported the synthesis of ordered macroporous TiO_2 film with mesoporous walls by using PS arrays

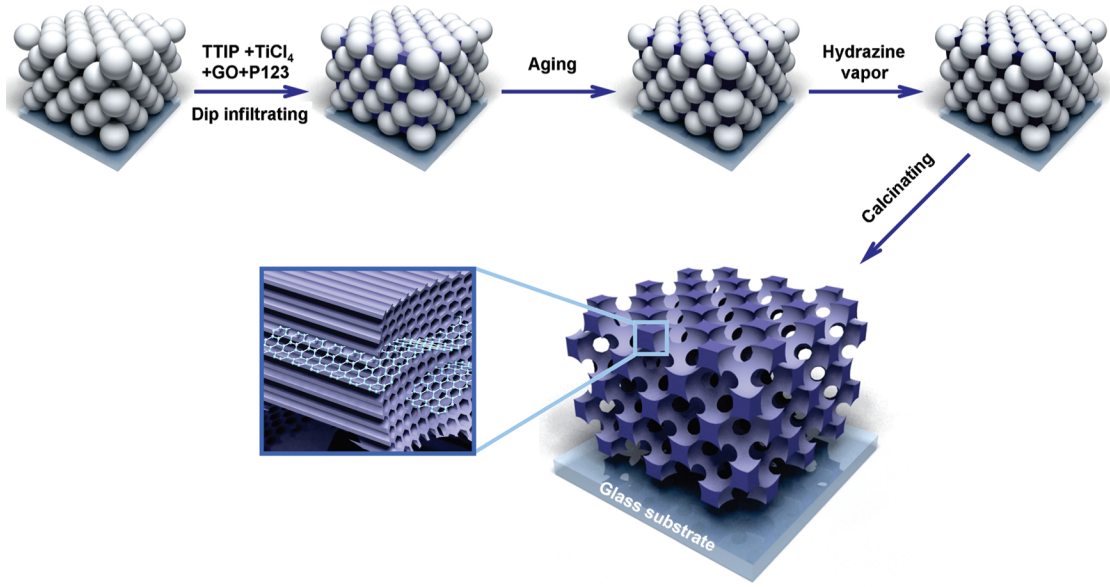

Scheme 1. Illustration for the preparation of macro−mesoporous TiO_2−graphene composite film.

as macropore templates and a triblock copolymer (Pluronic P123) as a mesopore template but only formed disordered mesostructures with a low specific surface area.[23] Nevertheless, it is still a challenge to independently control the porosity at each length scale to maximize the effectiveness of large pores and minimize the subsequent loss of surface area.

In this paper, we demonstrate the synthesis of hierarchically ordered macro−mesoporous titania films through a confinement self-assembly method within the regular voids of a three-dimensional (3D) periodic colloidal crystal, using Pluronic P123 and polystyrene spheres as a mesostructured template and a macrostructure scaffold, respectively. Macro−mesoporous titania films possess a well-ordered two-dimensional (2D) hexagonal (*p6mm*) mesostructure and well-interconnected periodic macropores as well as high specific surface areas and large pore volumes. Incorporation of interconnected macropores in mesoporous films significantly improves the mass transport through the film, reduces the length of the mesopore channel, and increases the accessible surface area within the thin film. Graphene has been selected as an example to incorporate with the hierarchically ordered macro−mesoporous titania frameworks. Because of the poor dispersion of graphene in the self-assembly system, we chose graphene oxide as a starting material and subsequently reduced it to graphene *in situ*. The results reveal that the composite photocatalysts based on this hierarchically ordered macro−mesoporous titania films demonstrate enhanced photodegradation of methyl blue (MB), confirming its superior photocatalytic activity.

RESULTS AND DISCUSSION

A pure mesoporous TiO_2 film (designated as Ti-Me) was prepared according to the evaporation-induced self-assembly procedure reported by Tian *et al.*,[12] except that the gelation process was carried out at a lower temperature to improve the mesostructural order. To obtain macro−mesoporous TiO_2 films, colloidal crystals assembled from monodisperse polystyrene spheres with controlled sizes (240 and 300 nm; the corresponding products were designated as Ti-Ma170-Me and Ti-Ma200-Me, respectively) were additionally used as the template for 3D ordered macropores. TiO_2−graphene composite films (designated as GR-Ti-Me, GR-Ti-Ma170-Me, and GR-Ti-Ma200-Me) were prepared by adding graphene oxide in the self-assembly system and subsequently reducing them *in situ* within the films (Scheme 1).

Figure 1 depicts the low-angle powder X-ray diffraction (XRD) patterns of a pure mesoporous titania film and macro−mesoporous titania films with and without graphene. All the XRD patterns have a sharp diffraction peak and two weaker peaks, which are characteristic of a 2D hexagonal (*p6mm*) structure.[24] Although the broadening of the (100) peaks in Figure 1, patterns b and c, confirms that the introduction of macropores breaks the long-range order of the mesostructure, two weaker, but obvious, (110) and (200) diffraction peaks

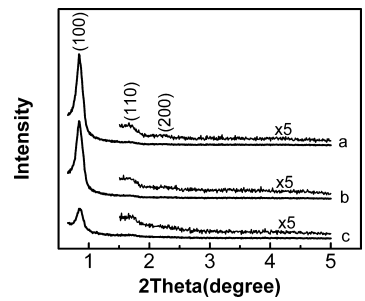

Figure 1. Low-angle XRD patterns of pure mesoporous titania film (Ti-Me) (a) and macro−mesoporous titania film (b) without and (c) with graphene (Ti-Ma200-Me and GR-Ti-Ma200-Me).

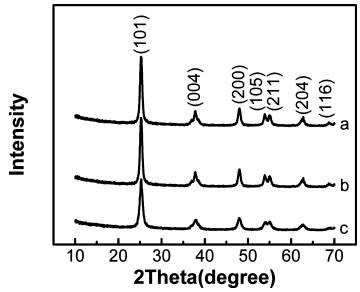

Figure 2. Wide-angle XRD patterns of pure mesoporous titania film (Ti-Me) (a) and macro−mesoporous titania films (b) without and (c) with graphene (Ti-Ma200-Me and GR-Ti-Ma200-Me).

indicate a highly periodic order with hexagonal symmetry in the resultant macro−mesoporous materials, as confirmed by the transmission electron microscope (TEM) images (see below). Wide-angle XRD clearly reveals that all the samples are anatase TiO_2 (Figure 2). No characteristic diffraction peaks of graphene in Figure 2, pattern c, were observed, possibly due to the reduced amount of graphene in the composite film (*ca.* 0.6 wt %).[25] Figure 3 shows XPS survey spectra of the macro−mesoporous films with and without graphene. The C 1s peak of macro−mesoporous film with graphene is stronger than that without graphene, confirming that the graphene was successfully introduced into macro−mesoporous films.[26]

Figure 4 shows typical electron microscope images of the as-prepared macro−mesoporous solid films compared with the pure mesoporous titania films. The SEM and TEM images show that 3D ordered macropores are formed. The periodic ordered macropores were derived from the colloidal crystal fabricated from 300 nm diameter PS spheres. The size of the hexagonally arrayed macropores (*ca.* 200 nm) in Figure 4a,b is smaller than that of their original template, which was due to the pyrolysis of the colloidal crystal template and subsequent shrinkage of macro−mesoporous frameworks during calcination processes. Three small holes of ~60 nm (indicated by black arrows in Figure 4a,b) are apparent inside every macropore, which derives from necks between the original PS spheres and also confirms that all the

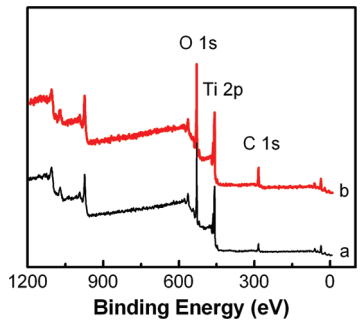

Figure 3. XPS survey spectra of macro−mesoporous titania films (a) without and (b) with graphene (Ti-Ma200-Me and GR-Ti-Ma200-Me).

macropores are well-interconnected. Higher-resolution TEM imaging (Figure 4g) reveals that the macropore wall consists of ~3 nm mesopores. The hexagonal and striped patterns (indicated by the white and black arrows), which viewed perpendicular to, and along the direction of, the hexagonal pore arrangement, respectively, confirm the periodic mesoporosity with hexagonal symmetry (*p6mm*), consistent with the low-angle XRD data. The striped pattern also reveals that the mesoporous channels confined within the macropore walls possess a shorter length (~100 nm) and completely run through macropore walls. In addition, the hexagonal and striped patterns were simultaneously captured along the same direction, revealing that the two domains have different directions of the hexagonal pore arrangement. Examination of multiple regions demonstrated that the direction of the mesoporous channels within the macropore wall is random.

The majority of the pores in the 2D hexagonal mesoporous thin films run parallel to the surface because the interfaces (substrate/film and film/air) prefer contact with either the hydrophilic or the hydrophobic part of the surfactants depending on the nature of the substrate.[12,27] For example, pure mesoporous TiO_2 films were prepared on a hydrophilic glass substrate without colloid crystals. These films demonstrated a very smooth top surface over tens of micrometers (Figure 4c) and longer mesoporous channels over 1 μm almost completely arranged parallel to the surface (Figure 4f,i). Unfortunately, these films are not very efficient photocatalysts due to the lack of access of mass into pores from the surface. However, there is a great difference in the formation of mesostructures within the regular confined voids of a colloidal crystal. The confined space and the interaction between surfactants and the hydrophilic surface of PS spheres disturb the preferred contact of the substrate surface and the surfactants, which not only shortens the pore channel length but also results in the random orientation of pore arrangement. This leads to the significant increase in the pore openings from the film surface and improvement of the accessibility of diffusing species to the films.

To evaluate the global photocatalytic activity of macro−mesoporous TiO_2, an investigation of the photocatalytic degradation of methylene blue (MB) in aqueous solution with the aforementioned titania films was performed.[28] The normalized temporal concentration changes (C/C_0) of MB during the photodegradation were proportional to the normalized maximum absorbance (A/A_0) and derived from the changes in the dye's absorption profile ($\lambda = 660$ nm) at a given time interval. Because the adsorption of organic molecules to the titania surface is a pivotal step in photocatalytic degradation, it is of great importance to investigate the adsorption characteristics of MB onto the surface of the differently prepared titania samples. The dark adsorp-

tion of MB of each film was monitored, and the remaining concentration fractions of MB after dark adsorption (see the experimental details in the Methods section) on the films were obtained from UV−visible absorption measurements (Figure 5). It was obvious that, after equilibrium in the dark for 20 min, most dye molecules (*ca.* 99.1%) remained in the solution with pure mesoporous titania film as the catalyst, whereas a large amount of dye molecules (*ca.* 16.9%) was adsorbed on the surface of the macro−mesoporous titania film Ti-Ma200-Me (see Table 1).

Because of the longer channels and smaller diameters of the mesopores as well as their parallel direction to the substrate, it is very difficult for MB not only to access the pure mesoporous titania films from the surface but also to reach the large amount of internal surface (Scheme S1, Supporting Information). In contrast to the aforementioned films, the length of mesopore channels in the macro−mesoporous films was effectively limited by the regular voids formed from the colloid crystals. In addition, the direction of these mesopore channels was random and the pore openings from the film surface also increased, significantly improving the accessibility of diffusing species (*i.e.*, MB) to the films, resulting in a larger adsorption of MB. The diameters of the periodic confined voids in the colloid crystals are related to the size of the templating PS spheres; therefore, macro−mesoporous films with shorter mesopore channels could be obtained by using colloid crystals composed of smaller polystyrene spheres, which are expected to supply more accessible surfaces. When a colloid crystal composed of 240 nm polystyrene spheres was used as the macroporous template, the resultant macro−mesoporous film (Ti-Ma170-Me) indeed shows a larger adsorption of MB (*ca.* 23.2%), verifying this assertion, although the periodic ordered mesostructure could not be maintained and the specific surface area also decreased slightly.

The photocatalytic activity of all the titania films can be quantitatively evaluated by comparing the apparent reaction rate constants, as illustrated in Figure 6. Direct comparison of the reaction rate constants between macro−mesoporous titania films (Ti-Ma170-Me and Ti-Ma200-Me) shows that they are markedly improved compared with that of pure mesoporous titania film (Ti-Me). In addition, their photocatalytic activities were increased 11 and 3 times, respectively, *versus* the pure, mesoporous titania film. This can be attributed to the significantly increased accessible surface area of the macro−mesoporous titania films, confirmed by their larger MB adsorption, almost 25 and 18 times larger, respectively, than that of the pure mesoporous titania film. After incorporating graphene into the macro−mesoporous titania films, the MB adsorption increased only slightly, while the apparent reaction rate constants increased 1.6 and 2.1 times, respectively, against macro−mesoporous films without graphene.

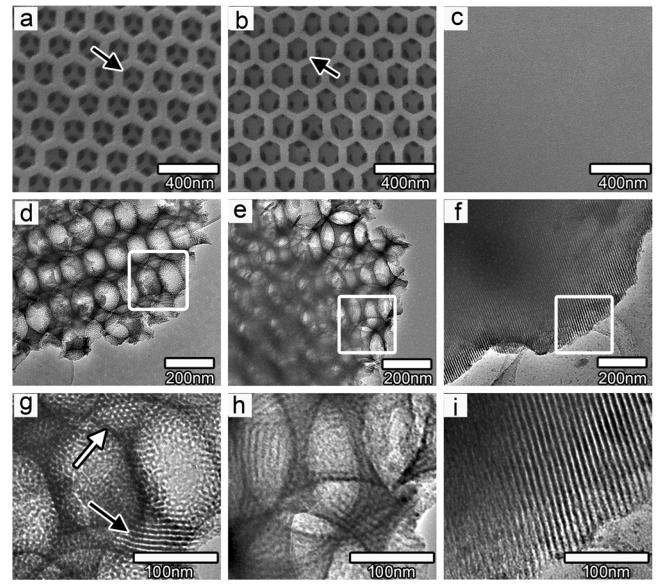

Figure 4. Typical SEM and TEM micrographs of macro−mesoporous titania films (a, d, g) without and (b, e, h) with graphene (Ti-Ma200-Me and GR-Ti-Ma200-Me) and pure mesoporous titania film (Ti-Me) (c, f, i). The black arrows in (a, b) indicate the interconnected channels between macropores in the films, whereas the white and black arrows in (g) suggest the mesopores in the macroporous walls.

This suggests that graphene within the macro−mesoporous titania films plays another role in the improvement of photocatalytic activity, that is, in accepting and transporting electrons. This results in the effective suppression of the recombination of photogenerated charge.

Previously, we have demonstrated that graphene incorporated into the titania anode of dye-sensitized solar cells could accept and rapidly transport the photogenerated electrons from the conduction band of titania, resulting in the reduction of charge recombination and the improvement of photoelectrical conversion efficiency.[26] In the macro−mesoporous titania−graphene composite films, graphene also serves as an acceptor of the photogenerated electrons from titania and effectively suppresses the charge recombination, leaving more photogenerated holes to form reactive species and facilitate the photodegrada-

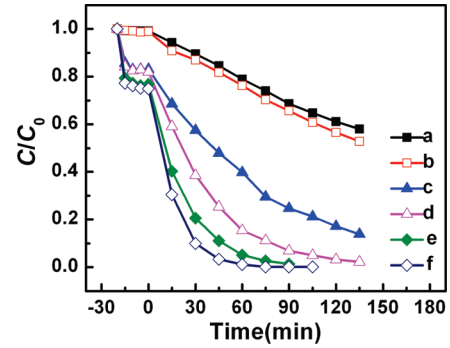

Figure 5. Photocatalytic degradation of MB under UV light irradiation using (a) Ti-Me, (b) GR-Ti-Me, (c) Ti-Ma200-Me, (d) GR-Ti-Ma200-Me, (e) Ti-Ma170-Me, and (f) GR-Ti-Ma170-Me films.

TABLE 1. Physical and Structural Properties of Selected Mesoporous and Macro−Mesoporous Samples

sample	S_{BET} ($m^2\ g^{-1}$)	$V_{mesopore}$ ($cm^3\ g^{-1}$)	pore size (nm)	adsorption of MB (%)	apparent reaction rate constants (min^{-1})
Ti-Me	299	0.57	2.9	0.9	0.0041
GR-Ti-Me	235	0.56	3.1	1.1	0.0047
Ti-Ma200-Me	298	0.56	3.0	16.9	0.013
GR-Ti-Ma200-Me	256	0.49	4.9	18.1	0.027
Ti-Ma170-Me	277	0.48	3.5	23.2	0.045
GR-Ti-Ma170-Me	215	0.49	4.2	25.1	0.071

tion of MB. To confirm the effect of graphene in transporting the electrons and restraining the recombination in the macro−mesoporous titania films, electrochemical impedance spectra (EIS), a powerful tool to clarify the electronic and ionic transport processes, were measured under the illumination of UV light at the open-circuit potential. Figure S1 (Supporting Information) shows the typical electrochemical impedance spectra of macro−mesoporous titania films with and without graphene. It is observed that the semicircle of medium frequencies in the plot became shorter after the introduction of graphene, which indicates a decrease in the solid-state interface layer resistance and the charge-transfer resistance on the surface.[5,26,29] Therefore, the electron-accepting and electron-transporting properties of graphene in the composite films could indeed suppress the charge recombination and improve their photocatalytic activities.

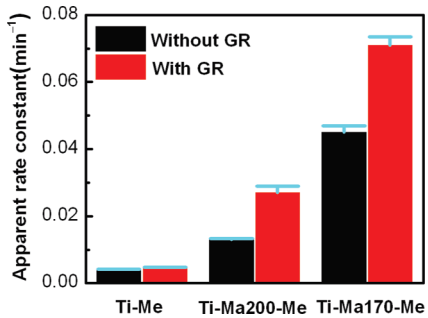

Figure 6. Comparison of the apparent rate constants of all the titania-based films.

CONCLUSIONS

In conclusion, we have successfully prepared hierarchically ordered porous titania films with two-dimensional (2D) hexagonal (*p6mm*) mesostructures and well-interconnected periodic macropores *via* a confinement self-assembly method. Incorporation of interconnected macropores in mesoporous films improves the mass transport through the film, reduces the length of the mesopore channel, increases the accessible surface area of the thin film, and significantly enhances their photocatalytic activities. Furthermore, graphene, as an excellent electron-acceptor and electron-transport material, was incorporated into the hierarchically ordered macro−mesoporous titania frameworks, effectively suppressing the charge recombination in the films. Hierarchically ordered macro−mesoporous TiO_2−graphene composite films show the enhanced capacity of rapidly adsorbing and photodegrading organic dyes, which are potentially suitable for wastewater treatment and air purification to remove organic pollutants and will provide an attractive opportunity for industrial applications.

METHODS

Synthesis of Graphene Oxide. Graphene oxide was synthesized from flake graphite (average particle diameter of 4 μm, Qingdao Tianhe Graphite Co. Ltd., Qingdao, China) by a modified Hummers method.[30] All other chemicals were of analytical reagent grade and used without further purification. Briefly, graphite powder (5 g) and $NaNO_3$ (3.75 g) were placed in a flask. Concentrated H_2SO_4 (375 mL) was then added slowly with stirring in an ice−water bath. $KMnO_4$ (22.5 g) was added gradually over 1 h under stirring and kept stirring for another 2 h. After stirring vigorously for 5 days at room temperature, the mixture was stirred at 35 °C for 2 h and then diluted with 5 wt % H_2SO_4 aqueous solution (700 mL) over 1 h. The mixture was then stirred at 98 °C for 2 h and then reduced to 60 °C, after which 30 wt % H_2O_2 (30 mL) was added, it was cooled to room temperature, and stirred for 2 h. The mixture was centrifuged and washed with an aqueous solution of 3 wt % H_2SO_4/0.5 wt % H_2O_2 (2 L) 15 times. The solids were washed with aqueous 3 wt % HCl (2 L) using a similar procedure and one additional wash with deionized H_2O (2 L). After adding another 2 L of deionized water and dispersing the solid using vigorous stirring and ultrasonication for 30 min, the final water solution was treated with a weak basic ion-exchange resin to remove the remaining HCl acid. The final solution was concentrated to 7.5 mg/mL.

Preparation of Macro−Mesoporous TiO_2−Graphene Composite Films. Polystyrene colloidal spheres were synthesized by a surfactant-free emulsion polymerization reaction as described elsewhere.[31] The polystyrene opal templates were settled on a glass substrate by the vertical deposition method.[32] The sol was prepared by mixing 1 g of Pluronic P123 ($EO_{20}PO_{70}EO_{20}$, M_{av} = 5800, Aldrich), dissolved in 20 g of ethanol or tetrahydrofuran (THF), with 0.6 g of $TiCl_4$ and 2.5 g of titanium isopropoxide. The mixture was stirred for 2 h. The pH value of the mother solution was *ca.* 1.2. A 1.25 mL portion of an aqueous suspension of graphene oxide (GO, 7.5 mg/mL) was added into the sol suspension (0.6 wt %). After that, it was stirred and dispersed in an ultrasonic cleaner for about 60 min so as to disperse GO within the suspension. The glass substrate covered with the polystyrene opal film was immersed vertically into the sol for 1 min. During the immersion process, the sol penetrates the voids in the template under the action of capillary forces. The gelation of the sol into the voids happened shortly after the template was pulled out of the solution, so the withdrawal rate was a critical factor in the whole infiltrated process. In our procedure, the withdrawal rate was 2.5 mm/s. The sample was then exposed to the atmosphere at 35 °C for 24 h to enable complete hydrolysis of the titania precursor. At last, the films were treated under hydrazine vapor at 40 °C for 24 h to reduce graphene oxide to graphene. After the

films were rinsed with deionized water and dried by heating to 40 °C in vacuum for 3 h, the films were annealed at 400 °C under argon for 3 h. The as-prepared films were then slowly heated in an oven (the heating rate was 5 °C/min) to 450 °C, held for 2 h at this temperature, and subsequently cooled slowly by turning off the oven. For comparison, pure mesoporous titania film and macro−mesoporous titania films were prepared *via* a similar procedure without adding graphene oxide in the sol.

Characterization. The XRD patterns were obtained by using an X'Pert PRO MDP with Cu Kα radiation (λ = 1.5405 Å) with 30 mA and 40 kV. XPS data were obtained with an ESCALab220i-XL electron spectrometer from VG Scientific using 300 W Al Kα radiation. SEM images were obtained using a JEOL JSM-6700F scanning electron microscope at 3.0 kV. The nitrogen adsorption and desorption isotherms at the temperature of liquid nitrogen (77 K) were measured on a Quantachrome Autosorb-1MP sorption analyzer with prior degassing under vacuum at 200 °C overnight. Total pore volumes were determined using the adsorbed volume at a relative pressure of 0.99. The multipoint BET surface area was estimated from the relative pressure range from 0.05 to 0.2. The pore size distributions were analyzed using the BJH algorithm. The EIS was carried out on a Zahner IM6e impedance analyzer (Germany) in the frequency range of 0.02 Hz to 100 kHz.

Photocatalytic Reactions. All the films were irradiated with UV light (24 W, λ = 365 nm) overnight to decompose pollutants adsorbed on its surfaces. The TiO_2 films (2.5 cm × 0.8 cm) were placed in a Petri dish filled with 0.01 mM MB aqueous solution (10 mL) in the dark for 20 min to allow the MB to adsorb onto the film surface. The photodegradation of MB was initiated and conducted by UV light irradiation without stirring. We monitored the absorbance of MB corresponding to I_{max} around 650−665 nm by UV−visible spectroscopy *versus* irradiation time (15 min intervals). The amount of MB decomposition was determined by a linear relationship between the concentration and the absorption of MB.

Acknowledgment. This work was partly supported by the National Natural Science Foundation of China (Nos. 21031005, 20971125, and 21006116), the Beijing Municipal Natural Science Foundation (No. 2082022), and the Foundation for State Key Laboratory of Multiphase Complex Systems and State Key Laboratory of Biochemical Engineering.

Supporting Information Available: Schematic illustration for the photodegradation of methylene blue over pure mesoporous titania film and macro−mesoporous titania film and EIS changes of macro−mesoporous titania films without and with graphene. This material is available free of charge *via* the Internet at http://pubs.acs.org.

REFERENCES AND NOTES

1. Bannat, I.; Wessels, K.; Oekermann, T.; Rathousky, J.; Bahnemann, D.; Wark, M. Improving the Photocatalytic Performance of Mesoporous Titania Films by Modification with Gold Nanostructures. *Chem. Mater.* **2009**, *21*, 1645–1653.
2. Yu, J. C.; Li, G. S.; Wang, X. C.; Hu, X. L.; Leung, C. W.; Zhang, Z. D. An Ordered Cubic *Im*3*m* Mesoporous Cr−TiO_2 Visible Light Photocatalyst. *Chem. Commun.* **2006**, 2717–2719.
3. Liu, G.; Chen, Z. G.; Dong, C. L.; Zhao, Y. N.; Li, F.; Lu, G. Q.; Cheng, H. M. Visible Light Photocatalyst: Iodine-Doped Mesoporous Titania with a Bicrystalline Framework. *J. Phys. Chem. B* **2006**, *110*, 20823–20828.
4. Wang, S.; Gong, Q. M.; Liang, J. Sonophotocatalytic Degradation of Methyl Orange by Carbon Nanotube/TiO_2 in Aqueous Solutions. *Ultrason. Sonochem.* **2009**, *16*, 205–208.
5. Zhang, H.; Lv, X. J.; Li, Y. M.; Wang, Y.; Li, J. H. P25-Graphene Composite as a High Performance Photocatalyst. *ACS Nano* **2010**, *4*, 380–386.
6. Abe, R.; Takami, H.; Murakami, N.; Ohtani, B. Pristine Simple Oxides as Visible Light Driven Photocatalysts: Highly Efficient Decomposition of Organic Compounds over Platinum-Loaded Tungsten Oxide. *J. Am. Chem. Soc.* **2008**, *130*, 7780–7781.
7. Ni, M.; Leung, M. K. H.; Leung, D. Y. C.; Sumathy, K. A Review and Recent Developments in Photocatalytic Water-Splitting Using TiO_2 for Hydrogen Production. *Renewable Sustainable Energy Rev.* **2007**, *11*, 401–425.
8. Tang, J.; Wu, Y. Y.; McFarland, E. W.; Stucky, G. D. Synthesis and Photocatalytic Properties of Highly Crystalline and Ordered Mesoporous TiO_2 Thin Films. *Chem. Commun.* **2004**, 1670–1671.
9. Pan, J. H.; Lee, W. I. Preparation of Highly Ordered Cubic Mesoporous WO_3/TiO_2 Films and Their Photocatalytic Properties. *Chem. Mater.* **2006**, *18*, 847–853.
10. Choi, H.; Antoniou, M. G.; Pelaez, M.; De la Cruz, A. A.; Shoemaker, J. A.; Dionysiou, D. D. Mesoporous Nitrogen-Doped TiO_2 for the Photocatalytic Destruction of the Cyanobacterial Toxin Microcystin-LR Under Visible Light Irradiation. *Environ. Sci. Technol.* **2007**, *41*, 7530–7535.
11. Grosso, D.; Soler-Illia, G.; Babonneau, F.; Sanchez, C.; Albouy, P. A.; Brunet-Bruneau, A.; Balkenende, A. R. Highly Organized Mesoporous Titania Thin Films Showing Mono-Oriented 2D Hexagonal Channels. *Adv. Mater.* **2001**, *13*, 1085–1090.
12. Tian, B. Z.; Yang, H. F.; Liu, X. Y.; Xie, S. H.; Yu, C. Z.; Fan, J.; Tu, B.; Zhao, D. Y. Fast Preparation of Highly Ordered Nonsiliceous Mesoporous Materials *via* Mixed Inorganic Precursors. *Chem. Commun.* **2002**, 1824–1825.
13. Crepaldi, E. L.; Soler-Illia, G.; Grosso, D.; Cagnol, F.; Ribot, F.; Sanchez, C. Controlled Formation of Highly Organized Mesoporous Titania Thin Films: From Mesostructured Hybrids to Mesoporous Nanoanatase TiO_2. *J. Am. Chem. Soc.* **2003**, *125*, 9770–9786.
14. Choi, S. Y.; Lee, B.; Carew, D. B.; Mamak, M.; Peiris, F. C.; Speakman, S.; Chopra, N.; Ozin, G. A. 3D Hexagonal (*R*-3*m*) Mesostructured Nanocrystalline Titania Thin Films: Synthesis and Characterization. *Adv. Funct. Mater.* **2006**, *16*, 1731–1738.
15. Liu, K. S.; Fu, H. G.; Shi, K. Y.; Xiao, F. S.; Jing, L. Q.; Xin, B. F. Preparation of Large-Pore Mesoporous Nanocrystalline TiO_2 Thin Films with Tailored Pore Diameters. *J. Phys. Chem. B* **2005**, *109*, 18719–18722.
16. Yang, P. D.; Deng, T.; Zhao, D. Y.; Feng, P. Y.; Pine, D.; Chmelka, B. F.; Whitesides, G. M.; Stucky, G. D. Hierarchically Ordered Oxides. *Science* **1998**, *282*, 2244–2246.
17. Zhang, L. Z.; Yu, J. C. A Sonochemical Approach to Hierarchical Porous Titania Spheres with Enhanced Photocatalytic Activity. *Chem. Commun.* **2003**, 2078–2079.
18. Dionigi, C.; Greco, P.; Ruani, G.; Cavallini, M.; Borgatti, F.; Biscarini, F. 3D Hierarchical Porous TiO_2 Films from Colloidal Composite Fluidic Deposition. *Chem. Mater.* **2008**, *20*, 7130–7135.
19. Kaune, G.; Memesa, M.; Meier, R.; Ruderer, M. A.; Diethert, A.; Roth, S. V.; D'Acunzi, M.; Gutmann, J. S.; Muller-Buschbaum, P. Hierarchically Structured Titania Films Prepared by Polymer/Colloidal Templating. *ACS Appl. Mater. Interfaces* **2009**, *1*, 2862–2869.
20. Sakamoto, J. S.; Dunn, B. Hierarchical Battery Electrodes Based on Inverted Opal Structures. *J. Mater. Chem.* **2002**, *12*, 2859–2861.
21. Meng, X. J.; Kimura, T.; Ohji, T.; Kato, K. Triblock Copolymer Templated Semi-Crystalline Mesoporous Titania Films Containing Emulsion-Induced Macropores. *J. Mater. Chem.* **2009**, *19*, 1894–1900.
22. Kimura, T.; Miyamoto, N.; Meng, X. J.; Ohji, T.; Kato, K. Rapid Fabrication of Mesoporous Titania Films with Controlled Macroporosity to Improve Photocatalytic Property. *Chem.—Asian J.* **2009**, *4*, 1486–1493.
23. Fu, Y. A.; Jin, Z. G.; Xue, W. J.; Ge, Z. P. Ordered Macro-Mesoporous Nc-TiO_2 Films by Sol-Gel Method Using Polystyrene Array and Triblock Copolymer Bitemplate. *J. Am. Ceram. Soc.* **2008**, *91*, 2676–2682.
24. Zhao, D. Y.; Feng, J. L.; Huo, Q. S.; Melosh, N.; Fredrickson,

G. H.; Chmelka, B. F.; Stucky, G. D. Triblock Copolymer Syntheses of Mesoporous Silica with Periodic 50 to 300 Angstrom Pores. *Science* **1998**, *279*, 548–552.
25. Li, J.; Liu, C. Y. Ag/Graphene Heterostructures: Synthesis, Characterization and Optical Properties. *Eur. J. Inorg. Chem.* **2010**, 1244–1248.
26. Yang, N. L.; Zhai, J.; Wang, D.; Chen, Y. S.; Jiang, L. Two-Dimensional Graphene Bridges Enhanced Photoinduced Charge Transport in Dye-Sensitized Solar Cells. *ACS Nano* **2010**, *4*, 887–894.
27. Lee, U. H.; Kim, M. H.; Kwon, Y. U. Mesoporous Thin Films with Accessible Pores From Surfaces. *Bull. Korean Chem. Soc.* **2006**, *27*, 808–816.
28. Ryu, J.; Choi, W. Substrate-Specific Photocatalytic Activities of TiO_2 and Multiactivity Test for Water Treatment Application. *Environ. Sci. Technol.* **2008**, *42*, 294–300.
29. He, B. L.; Dong, B.; Li, H. L. Preparation and Electrochemical Properties of Ag-Modified TiO_2 Nanotube Anode Material for Lithium-Ion Battery. *Electrochem. Commun.* **2007**, *9*, 425–430.
30. Becerril, H. A.; Mao, J.; Liu, Z.; Stoltenberg, R. M.; Bao, Z.; Chen, Y. Evaluation of Solution-Processed Reduced Graphene Oxide Films as Transparent Conductors. *ACS Nano* **2008**, *2*, 463–470.
31. Goodwin, J. W.; Hearn, J.; Ho, C. C.; Ottewill, R. H. Studies on Preparation and Characterization of Monnodisperse Polystyrene Lattices. III. Preparation without Added Surface-Active Agents. *Colloid Polym. Sci.* **1974**, *252*, 464–471.
32. Nishimura, S.; Abrams, N.; Lewis, B. A.; Halaoui, L. I.; Mallouk, T. E.; Benkstein, K. D.; van de Lagemaat, J.; Frank, A. J. Standing Wave Enhancement of Red Absorbance and Photocurrent in Dye-Sensitized Titanium Dioxide Photoelectrodes Coupled to Photonic Crystals. *J. Am. Chem. Soc.* **2003**, *125*, 6306–6310.